Photoelectrocatalysis of Hydrogen Peroxide at Functionalized Multi-Walled Carbon Nanotubes (*f*-MWCNT) with Brilliant Blue Modified Electrode

Ying Li, Cheng-Yu Yang, Shen-Ming Chen[*]

Department of Chemical Engineering and Biotechnology, National Taipei University of Technology, No.1, Section 3, Chung-Hsiao East Road , Taipei 106, Taiwan (R.O.C).
[*]E-mail: smchen78@ms15.hinet.net

f-MWCNTs/BB modified electrode which contains functionalized multi-walled carbon nanotubes (*f*-MWCNTs) and Brilliant blue FCF (BB) has been synthesized on glassy carbon electrode (GCE) and indium tin oxide (ITO). The presence of *f*-MWCNTs enhances the surface coverage (Γ) and stability in the pH range between 1.0 to 13. Electrochemical impedance spectra (EIS) was applied to monitor the whole process of the electrode modification. UV–visible absorption spectra results confirmed that the *f*-MWCNTs/BB film was successfully eletropolymerization on the electrode surface. We have studied the surface morphology of the modified electrode using scanning electron microscopy (SEM) and atomic force microscopy (AFM), which revealed that BB is coated on *f*-MWCNTs. The cyclic voltammetrys (CVs) has been used for the measurement of electroanalytical properties of analytes by means of modified electrodes. The sensitivity values of *f*-MWCNTs/BB modified glassy carbon electrode are higher than the values which are obtained for only BB film and *f*-MWCNTs modified electrode. Finally, the amperometry method has been used for the detection of hydrogen peroxide at *f*-MWCNTs/BB modified electrode under stirred condition. The *f*-MWCNTs/BB modified electrode also exhibits a promising enhanced photoelectrocatalytic activity for hydrogen peroxide under illumination.

1. INTRODUCTION

Brilliant blue FCF (BB, Blue 1, CI 42090) [1], a food processing dye, were selected as the model compounds to determine the interactions between dye and surfactant molecules. BB is also commonly used in cosmetics, textile, leather, paper and ink industries. Light has been used in the chemical treatment of water since many years. In all cases, direct action of light is limited due to the

absorption spectra of pollutants to be degraded. Thus, direct photochemical reaction has given a way to a sensitized photochemical or photoassisted reaction [2-5]. Dye mediated photocatalysis is a promising method for the complete removal of a variety of environmental contaminants, such as hydrogen peroxide. It is well reported that the catalyst possess electrocatalytical activity when illuminated with UV or solar irradiation. In photocatalytic reactions, the formation of electron-hole pair on a photo-illuminated catalyst surface is one of the key steps. To the best of our knowledge, there were many reports about the hydrogen peroxide solution as co-photocatalysts with dye [6].

As an environmentally and biochemically relevant species, hydrogen peroxide is considered as the most efficient oxidant for the conversion of dissolved sulphur dioxide to sulphuric acid which is one of main contributors to the acidification of rain water [7]. Besides, H_2O_2 is a widely used chemical reagent as an essential mediator in many fields such as food, pharmaceutical, clinical and bleaching-related industries. The oxidative damage resulting from cellular imbalance of H_2O_2 is connected to aging and severe human diseases. It is a weak acid with strong oxidising properties and is inexpensive and readily available for use as a common bleaching agent and disinfectant [8]. As a consequence, intense research efforts have been directed to develop the analytical methods for the detection of H_2O_2 [9-10], such as amperometry [11-13], differential pulse voltammetry (DPV) [14], fluorimetry [15] and chemiluminescence [16]. A number of spetrophotometry methods have been proposed for the determination of H_2O_2 [17-18]. However, most of them are based on peroxidase-catalysis reaction and their application is limited due to the reliance of instable and high cost of enzymes such as horseradish peroxidase.

Small particles tend to aggregate, resulting in lower or even completely lost photocatalytic activity. For example, nanosized TiO_2 is one of the most promising photocatalysts. To achieve high activities in solution-phase catalysis the dispersion of the catalyst is very important [19]. Varieties of applications of carbon nanotubes (CNT) with dye were already reported [20-22]. Even though, electrocatalytic activity of the conjugated dye and CNTs matrices individually shows good result; some properties like mechanical stability, sensitivity for different techniques and electrocatalysis of multiple compounds are found to be poor.

This paper discusses the photoelectrochemistry of Brilliant blue films composed of CNTs matrices on various electrodes, and the enhancement of the electropolymerization by *f*-MWCNTs modification of the electrode surface. Two-layer modified electrodes were prepared from Brilliant blue and *f*-MWCNTs films. Brilliant blue films were photoelectrocatalytically active for hydrogen peroxide.

2. EXPERIMENTAL

2.1. Materials

Multi-walled carbon nanotubes (Aldrich) was used as received. Brilliant blue FCF (BB) (Everlight Chemical Industrial Co., Ltd, Taiwan) and hydrogen peroxide (H_2O_2) were used as received. All other chemicals used were of analytical grade and used without further purification. Aqueous solutions of pH 7.0 were prepared using 0.1 M phosphate buffer solutions (PBS). Where pH 1.0 and

1.5 were prepared using sulfuric acid (H_2SO_4). All the solutions were prepared using doubly distilled deionized water and then deaerated by purging with high purity nitrogen gas for about 20 min before performing electrochemical experiments. Also, a continuous flow of nitrogen over the aqueous solution was maintained during measurements.

2.2. Apparatus

The electrochemical measurements were performed with a CH Instruments (Model CHI-627 and CHI-1205A) using CHI-750 potentiostat. Cyclic voltammetric studies were carried out with a BAS glassy carbon electrode (GCE; area 0.07 cm^2) while amperometric measurements were performed using PINE GCE (0.19 cm^2). A platinum wire served as counter electrode and an Ag / AgCl (sat KCl) reference electrode was used to monitor the cell potentials. Prior to modification, GC electrode was polished with 0.05 μm alumina on Buehler felt pads and then ultrasonically cleaned for about a minute in water. Finally, the electrode was washed thoroughly with double distilled water and dried at room temperature. The morphological characterizations of the films were examined by means of SEM (Hitachi S-3000H) and atomic force microscopy (AFM) (Being Nano-Instruments CSPM5000). Electrochemical impedance spectroscopy (EIS) measurements were performed using an IM6ex Zahner instrument (Kroanch, Germany). The UV-visible absorption spectra were checked by using a U3300 Spectrophotometer (HITACHI). All the experiments were carried out at room temperature ($\approx$ 25°C).

2.3. Preparation of modified electrode

2.3.1 Preparation of f- MWCNTs

The produced functionalized multiwall carbon nanotubes (*f*-MWCNTs) were suspended in a concentrated sulfuric acid–nitric acid mixture (3:1 v/v) and sonicated in a sonication bath for 2 h. A nanotube mat was obtained after filtration using a 0.45 mm hydrophilized PTFE membrane and washed with deionized water until no acid was detected, followed by drying under vacuum [23]. Thus obtained *f*-MWCNTs 10 mg in 10 ml water was ultrasonicated for 6 hr to get a uniform dispersion. This functionalization process of *f*-MWCNTs was done to get a hydrophilic nature for the homogeneous dispersion, in water. This process not only converts *f*-MWCNTs to hydrophilic nature but this helps to breakdown larger bundles of *f*-MWCNTs in to smaller ones also [24].

2.3.2. Preparation of Glassy Carbon Electrodes Modified with f-MWCNTs/BB

Prior to modification, glassy carbon electrode was polished with 0.05 μm alumina on Buehler felt pads and then ultrasonically cleaned for about a minute in water. Finally, the electrode was washed thoroughly with double distilled water and dried at room temperature. The cleaned glassy carbon electrode was coated with 2μL of *f*-MWCNTs and the solvent allowed evaporating at room temperature. The electropolymerization of Brilliant blue FCF (BB) was done by electrochemical

oxidation of Brilliant blue FCF (BB) 1×10^{-3} M on the *f*-MWCNT modified glassy carbon electrode using pH 1.5 H_2SO_4. It was performed by consecutive Cyclic voltammetrys over a suitable potential range of -0.7 to 1.2 V; scan rate = 100 mVs^{-1}. The optimization of poly- Brilliant blue FCF (BB) growth potential has been determined by various studies with different electropolymerization potentials. After film formation, the electrode was rinsed with distilled water and used for further characterization.

3. RESULTS AND DISCUSSIONS

3.1. Electrochemical characterizations of f-MWCNTs/BB film
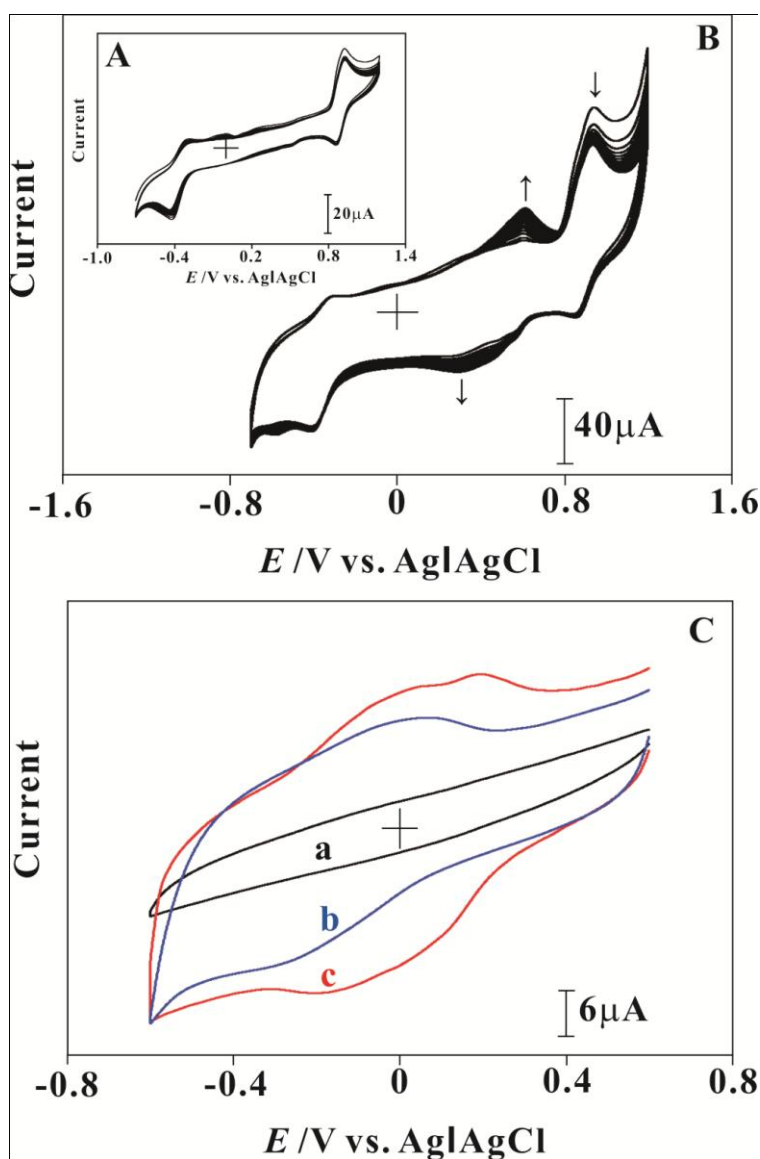
Figure 1. Repetitive Cyclic voltammograms of (A) only BB film, (B) *f*-MWCNTs/BB modified from 1×10^{-3} M BB in pH 1.5 H_2SO_4 buffer, scan rate at 100 mVs^{-1}. (C) Comparison of Cyclic voltammograms (a) only BB film, (b) *f*-MWCNTs and (c) *f*-MWCNTs/BB films on GCE in pH 7.0 PBS buffer, scan rate at 100 mVs^{-1}.

The electrochemical formation of a film of adhered Brilliant blue FCF (BB) on a glassy carbon electrode (GCE) along with enhanced electropolymerization by a *f*-MWCNTs modified electrode was performed using consecutive cyclic voltammetry between suitable potentials in strongly acidic aqueous solutions (pH 1.5 aqueous H_2SO_4 solution). The former film was prepared using electrochemical oxidation with an anodic wave current occurring between the potentials of -0.7 to 1.2 V. Figure 1 (A) showed the only BB film growth of the cyclic voltammetrys current exhibiting a redox couple with a formal potential of $E^{0'} = 0.68$ V (vs. Ag|AgCl). The increase in peak current at the redox couple indicates that film formation occurred. The second type of electrochemical film formation arising from the adherence of BB on a *f*-MWCNTs modified glassy carbon electrode was performed using consecutive cyclic voltammetrys between the same conditions. Figure 1 (B) the redox couple showed a larger growth in peak current than only BB film. The growth in the cyclic voltammetric current showed that the redox couple occurred at a formal potential of $E^{0'} = 0.45$ V (vs. Ag|AgCl). The more rapid increase in peak current, and the larger magnitude of the peak current of the redox couple in Figure 1 (B), indicates that film formation occurred, and that this was enhanced by the *f*-MWCNTs on the modified electrode surface. Brilliant blue FCF (BB) films could also be synthesized in strong acidic aqueous solutions using consecutive cyclic voltammetrys on ITO electrodes that had been modified by including *f*-MWCNTs on the electrode surface.

Table. 1. Surface coverage (Γ) of Brilliant blue FCF (BB) at glassy carbon modified electrode.

Electrode type	Modified film	Γ (mol cm^{-2})
GCE [a]	Brilliant blue FCF (BB)	4.74×10^{-13}
	f-MWCNTs	2.68×10^{-11}
	f-MWCNTs/BB	4.11×10^{-11}

In the following experiments, each newly prepared film on glassy carbon electrode has been washed carefully in deionized water to remove the loosely Brilliant blue FCF (BB) on the modified glassy carbon electrode. It was then transferred to pH 7.0 PBS solution for the other electrochemical characterizations. These optimized pH solutions have been chosen to maintain the higher stability (pH = 7.0). Figure 1 (C) showed different types (a) only BB film, (b) *f*-MWCNTs and (c) *f*-MWCNTs/BB. The corresponding cyclic voltammetric have been measured at 100 mVs^{-1} scan rate in the potential range of 0.6 to -0.6 V. From Figure 1 (C), a pair of well defined redox peak has been observed at formal potential ($E^{0'}$) = 0.18 V (vs. Ag|AgCl) for *f*-MWCNTs/BB film (curve c). However, no peaks at only BB film (curve a). Similar results have been observed at ITO electrodes (figure not shown). Comparison of curve (a) and curve (c), it is found that the presence of *f*-MWCNTs showed the catalytic effect on Brilliant blue FCF (BB) redox peak currents. Further, it has been observed that the presence of *f*-MWCNTs increases the overall back ground current, which is similar to that of previous studies [25-26]. These above results showed that, Brilliant blue FCF (BB) exhibits reversible redox peaks only in the presence of *f*-MWCNTs at various electrodes. The surface coverage (Γ) values for Brilliant blue FCF (BB) at different modified electrodes have been calculated and given in Table 1.

The Γ value has been applied in the equation : $\Gamma = Q/nFA$. where Q is the charge, n is the number of electrons involved, F, Faraday current and A, electrode area. Where the number of electrons transferred is two. We can note the enhanced Γ of Brilliant blue FCF (BB) in the *f*-MWCNTs modified electrode. These values indicate that the presence of *f*-MWCNTs increased the surface area of the electrode, which in turn has increased the Γ of Brilliant blue FCF (BB). The calculated values from the same table showed that, the overall percentage of increase in Γ of Brilliant blue FCF (BB) in *f*-MWCNTs film is 1.43×10^{-11} mol cm^{-2}.
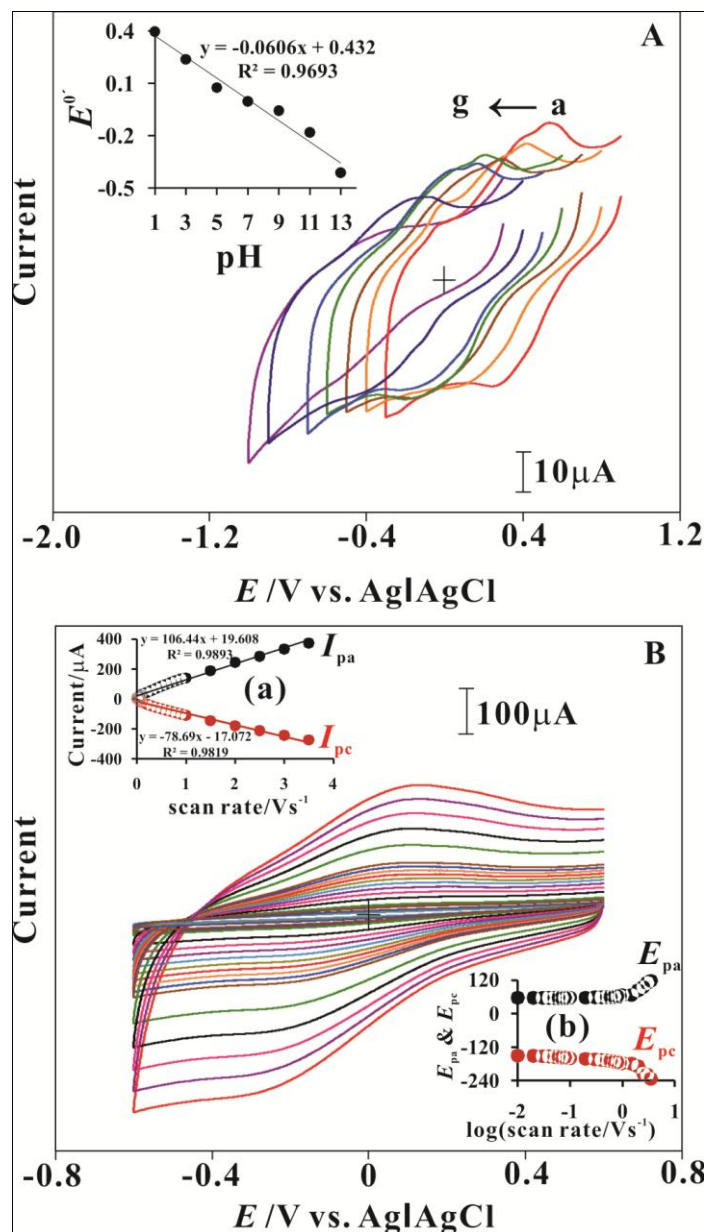

Figure 2. (A) Cyclic voltammograms of the *f*-MWCNTs/BB transferred to various pH solutions (a) 1; (b) 3; (c) 5; (d) 7; (e) 9; (f) 11; (g) 13. The inset shows the formal $E^{0'}$ vs. pH. (B) Cyclic voltammograms of pH 7.0 PBS at *f*-MWCNTs/BB electrode at different scan rate from 10 mV s^{-1} to 3500 mV s^{-1}, respectively. Calibration curve for data in (a) shows I_{pa} & I_{pc} vs. scan rate; (b) E_{pa} & E_{pc} vs. log(scan rate).

Figure 2 (A) showed the cyclic voltammetric of *f*-MWCNTs/BB on electrode obtained in pH 1.5 aqueous H_2SO_4 solution, then washed with deionized water and was transferred to various pH aqueous buffer solutions. This showed that the film is highly stable in the pH range between 1.0 to 13. The values of E_{pa} and E_{pc} depends on the pH value of the buffer solution. The inset in Figure 2 (A) showed the potential of *f*-MWCNTs/BB plotted over a pH range from 1.0 to 13. The response showed a slope of -60 mV/pH, which is close to that given by the Nernstian equation for equal number of electrons and protons transfer [27-28]. The values of $E^{0'}$, which depend on the pH, also showed that the redox couple of the polymeric film includes proton transfer in the reduction and oxidation processes. The chemical composition and possible electropolymerization of a Brilliant blue FCF (BB) film is analogous to that of polyaniline and its analogues [29-34].

Figure 2 (B) showed that the *f*-MWCNTs/BB film on a glassy carbon electrode had one chemically reversible redox couple at 0.18 V in the pH 7.0 PBS when cyclic voltammetry was performed at different scan rates (10 to 3500 mVs^{-1}). The anodic and cathodic peak currents of both the film redox couples which have increased linearly with the increase of scan rates. The inset calibration curve for data in Figure 2 (B) showed (a) I_{pa} & I_{pc} vs. scan rate, (b) E_{pa} & E_{pc} vs. log (scan rate). The ratio of I_{pa}/I_{pc} from the inset has demonstrated that the redox process has not been controlled by diffusion. This behavior perhaps occurs because of a reversible electron transfer process involving the Brilliant blue FCF (BB) on the *f*-MWCNTs layer, with a proton exchange process occurring along with the electron transfer process. However, the ΔE_p of each scan rate reveals that the peak separation of composite redox couple increases as the scan rate is increased.

3.2. Electrochemical impedance spectra (EIS) of analysis

Electrochemical impedance spectra (EIS) was applied to monitor the whole process of the electrode modification. EIS can give useful information of the impedance changes on the electrode surface between each step. Figure 3 (A) showed the results of EIS for different type modified electrodes in the presence of equimolar 5 mM $[Fe(CN)_6]^{3-/4-}$ in pH 7.0 PBS. The EIS includes a semicircular part and a linear part. The semicircular part at higher frequencies corresponds to the electron transfer limited process and the diameter is equivalent to the electron transfer resistance (R_{ct}). The linear part at lower frequencies corresponds to the diffusion process. During the fabrication, significant differences were observed. R_{ct} of a bare GCE is 941 Ω (curve b). The GCE was modified with Brilliant blue FCF (BB), R_{ct} value was increased dramatically (figure not shown). R_{ct} of a *f*-MWCNTs is 1526 Ω (curve c). EIS results for the electrode modified with the *f*-MWCNTs/BB are showed in curve a and R_{ct} was considerably increased to 1560 Ω. These results confirmed that the *f*-MWCNTs/BB film was successfully immobilized on the GCE surface. From these observations, we can conclude that the *f*-MWCNTs were highly conductive and expected as a good platform for sensing applications.
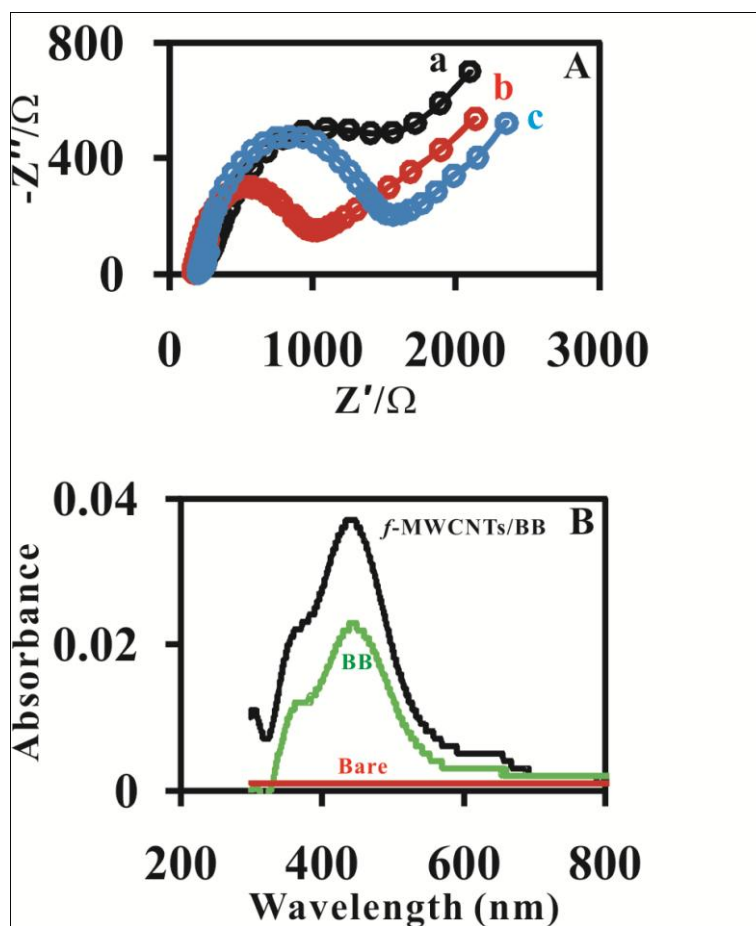
Figure 3. (A) Electrochemical impedance spectra (EIS) of (a) *f*-MWCNTs/BB; (b) bare GCE and (c) *f*-MWCNTs in pH 7.0 PBS containing 5×10^{-3} M $[Fe(CN)_6]^{-3/-4}$ (Amplitude: 5 mV). (B) UV–vis absorption spectra of *f*-MWCNTs/BB, only BB film and bare modified on ITO electrode.

3.3. UV–visible absorption spectra of analysis

Figure 3 (B) showed the UV–visible absorption spectra for electropolymerization only BB film, *f*-MWCNTs/BB and bare modified ITO electrodes. For the electropolymerization *f*-MWCNTs/BB film (black line), a strong UV absorption peak centered at 448 nm has been noticed corresponds to the presence of *f*-MWCNTs on the ITO surface. For only BB film (green line), UV absorption peak appears at 459 nm. Therefore, the absorption peak shift slightly validates the *f*-MWCNTs/BB. Finally, the UV spectrum studies clearly represent the presence of *f*-MWCNTs can enhance intensity of the absorption. These results confirmed that the *f*-MWCNTs/BB film was successfully immobilized on the ITO surface.

### 3.4. Morphological characterization of f-MWCNTs/BB film

Figure 4 represents the top view SEM images of different films coated on ITO surfaces taken at a resolution. In prior to modification, ITO surfaces were cleaned and ultrasonicated in acetone–water mixture for 15 min and then dried. Only BB film, *f*-MWCNTs and *f*-MWCNTs/BB have been prepared

on the ITO electrode. From Figure 4, it is significant that there are morphological differences between both the films. The top views of structures Figure 4 (A) on the ITO electrode surface showed only BB film on this electrode. Figure 4 (B) was *f*-MWCNTs top view. The *f*-MWCNTs/BB film in Figure 4 (C) reveals that the BB had covered the entire *f*-MWCNTs to form *f*-MWCNTs/BB modified electrode. The same modified ITO electrodes have been used to measure the AFM topography images of Figure 5 (A) only BB film, (B) *f*-MWCNTs and (C) *f*-MWCNTs/BB electrode. In all these cases the observed morphological structure is similar to that of SEM.
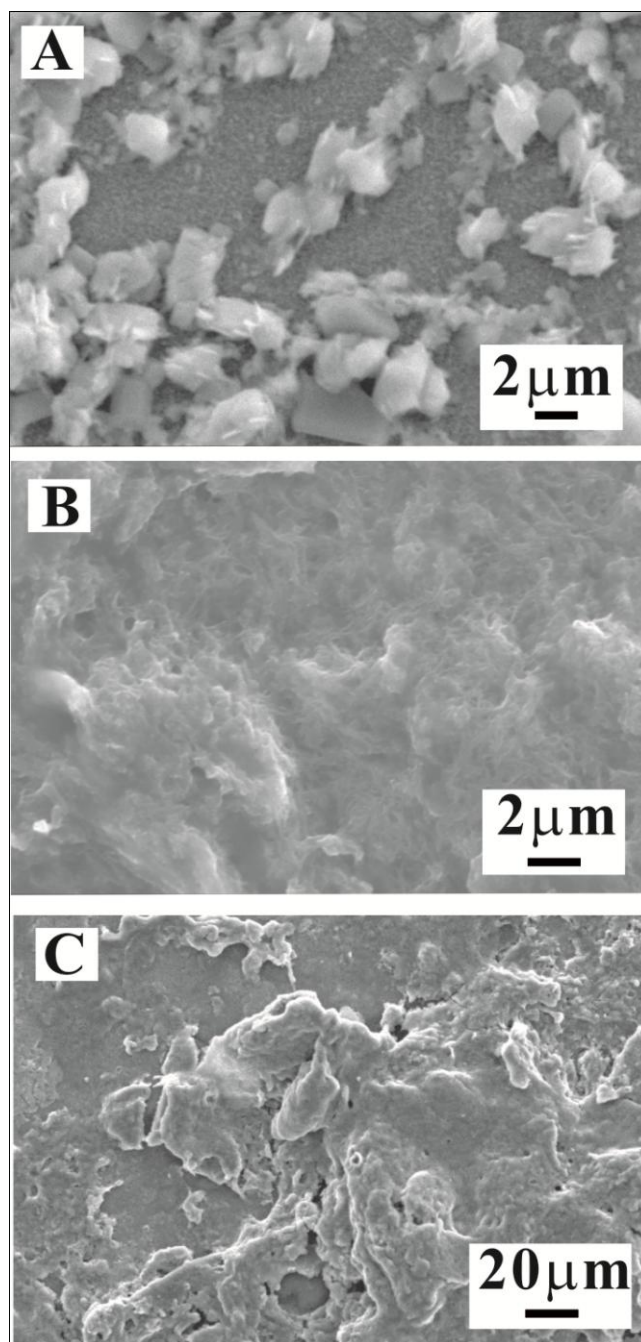
Figure 4. SEM images of (A) only BB film; (B) *f*-MWCNTs and (C) *f*-MWCNTs/BB on ITO electrode.
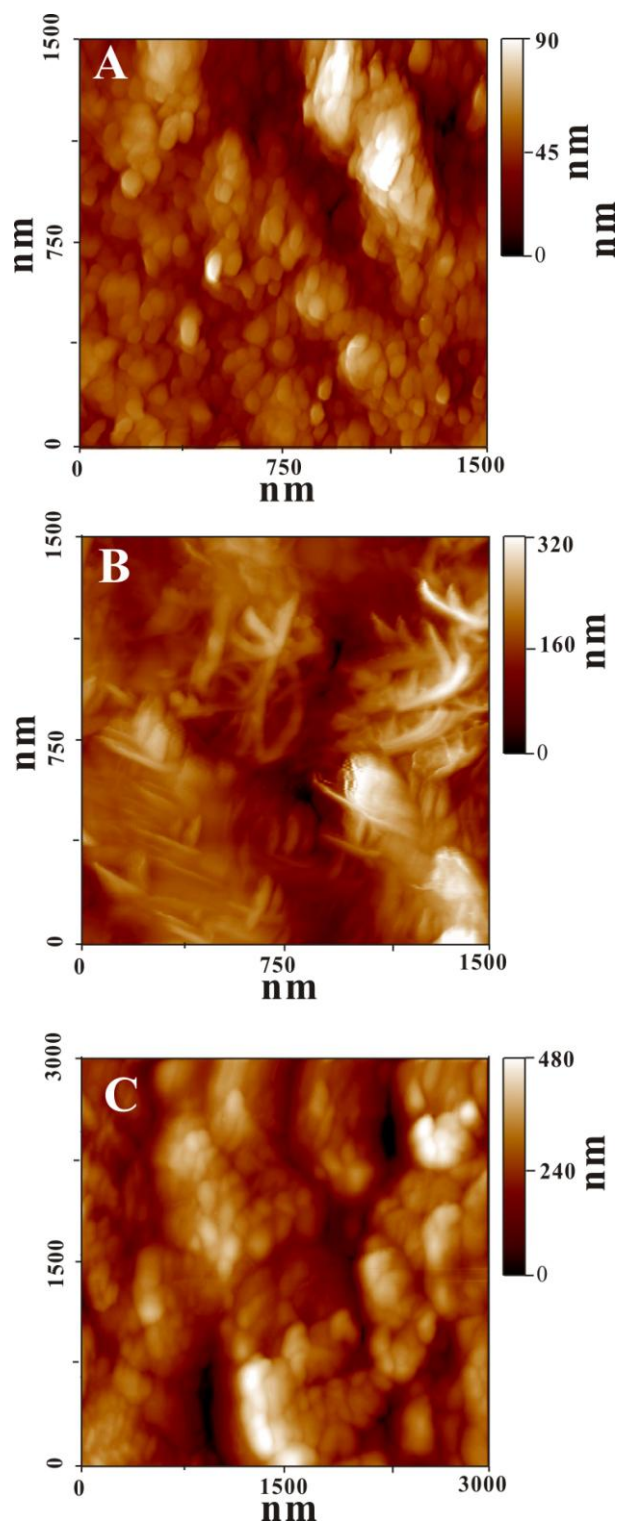
Figure 5. AFM images of (A) only BB film; (B) *f*-MWCNTs and (C) *f*-MWCNTs/BB on ITO electrode.

3.5. Electrocatalytic response of hydrogen peroxide

Figure 6 (A) showed the electrocatalytic response of hydrogen peroxide by Cyclic voltammograms, at *f*-MWCNTs/BB with a scan rate of 100 mVs^{-1}. In Figure 6 (A), curve (a) is the *f*-

MWCNTs/BB in pH 7.0 PBS; curve (a') represents bare GCE and curve (b) is *f*-MWCNTs/BB both at the highest concentrations of hydrogen peroxide (1.1 mM). The cyclic voltammetric for *f*-MWCNTs/BB exhibit a reversible redox couple in the absence of hydrogen peroxide, and on the addition of analytes a new growth in the response peak of analytes appeared at E_{pa} = -0.45 V.
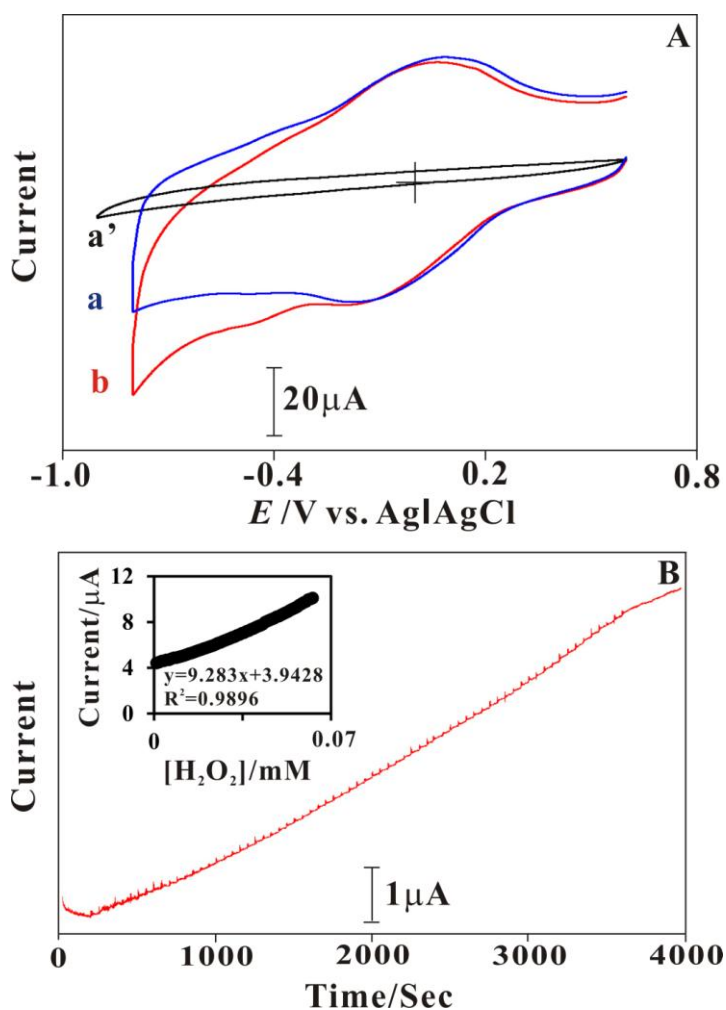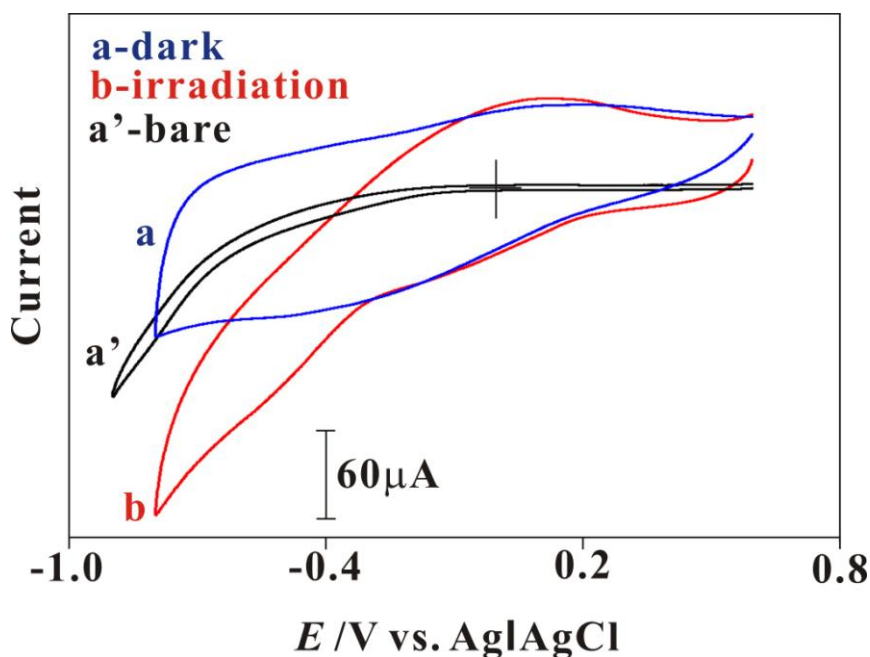

Figure 6. (A) The electrocatalytic of hydrogen peroxide by Cyclic voltammograms, at *f*-MWCNTs/BB modified GCE with a scan rate of 100 mV s^{-1}. (a) and (b) *f*-MWCNTs/BB are absence and presence hydrogen peroxide in pH 7.0 PBS; (a') bare GCE at the highest concentrations of hydrogen peroxide (1.1 mM). (B) Amperometric response at *f*-MWCNTs/BB electrode to the successive injection of 100 μL of 10 mM hydrogen peroxide. Applied potential -0.45 V. Rotation rate: 1000 rpm. Insert shows different concentration vs. current.

The detection limit of *f*-MWCNTs/BB modified electrodes for hydrogen peroxide was 0.09 mM. The sensitivity of *f*-MWCNTs/BB modified electrodes was 160.1 μA mM^{-1} cm^{-2}. More specifically, the enhanced electrocatalysis of *f*-MWCNTs/BB can be explained in terms of higher peak current than that of *f*-MWCNTs and both lower overpotential and higher peak current than that of only BB film, where the increase in peak current and lower overpotential both are considered as the electrocatalysis [35]. It is obvious (figure not shown) that the sensitivity of *f*-MWCNTs/BB is higher

for analytes when compared with *f*-MWCNTs and only BB film. The overall view of these results clearly reveals that *f*-MWCNTs/BB is efficient for s hydrogen peroxide detection.

In order to utilize the *f*-MWCNTs/BB have been synthesized on GCE for hydrogen peroxide determination, amperometry under stirred condition was used in the further investigation to construct calibration curve. Figure 6 (B) showed amperograms obtained by holding the potential of *f*-MWCNTs/BB film electrode at -0.45V and successive injection of 100 μL of 10 mM hydrogen peroxide to pH 7.0 PBS supporting electrolyte. For each addition, a well defined current response was obtained. As showed in figure 6 (B), the current in whole concentration range, 9.9×10^{-7} to 1.1×10^{-3} M. The sensitivity of *f*-MWCNTs/BB film electrode was found to be 48.85 μA mM^{-1} with a correlation coefficient of 0.9896. The sensor achieves 98% of steady-state current in less than 5 s. Such a short response time indicates fast mass transfer across the film and also fast electron exchange between *f*-MWCNTs and analyte.

3.6. photoelectrocatalytic responses of the hydrogen peroxide at f-MWCNTs/BB

Figure 7. The photoelectrocatalytic of hydrogen peroxide by Cyclic voltammograms, at *f*-MWCNTs/BB modified ITO electrode (1×1 cm^2) with scan rate 100 mVs^{-1}. Light source, Xe lamp (100 mWcm^{-2}). (a) unirradiation and (b) irradiation with *f*-MWCNTs/BB film in 1.1 mM hydrogen peroxide in pH 7.0 PBS; (a') bare GCE in the of hydrogen peroxide (1.1 mM) at irradiation.

A typical photocurrent response of *f*-MWCNTs/BB film modified ITO electrode (area : 1×1 cm^2) with scan rate 100 mVs^{-1} under illumination (light source, Xe lamp 100 mWcm^{-2}) by Cyclic voltammograms is presented in Figure 7. As the figure indicates, a broad background current was first observed for the response of *f*-MWCNTs. With the injection of a higher hydrogen peroxide concentration, the photocurrent increases with the increase of concentration. In figure curve (a) and (b)

were *f*-MWCNTs/BB in 1.1 mM hydrogen peroxide in pH 7.0 PBS; curve (a') was bare GCE in hydrogen peroxide (1.1 mM) at irradiation. Comparison of curve (a) and curve (b), it is found increased the photocatalytic effect of peak currents under illumination. Above these results validates that the *f*-MWCNTs/BB modified electrode is capable for the electro catalytic response of hydrogen peroxide in lower and higher concentration ranges.

4. CONCLUSIONS

We have demonstrated application of *f*-MWCNTs/BB modified electrode for determination of hydrogen peroxide. It is found increased the catalytic effect of peak currents under illumination. The modified electrode showed stable response. This feature provides a favorable for fule cell at electrocatalytic response of hydrogen peroxide under illumination. High sensitivity and stability together with very easy preparation makes *f*-MWCNTs/BB electrode as promising candidate for constructing simple electrochemical sensor for hydrogen peroxide determination. The SEM and AFM results have showed the difference between *f*-MWCNTs and *f*-MWCNTs/BB films morphological data. Further, it has been found that the *f*-MWCNTs/BB has an excellent functional property along with good photoelectrocatalytic activity on hydrogen peroxide. The experimental methods of Cyclic voltammograms and amperometry with film biosensor integrated into the GCE and ITO which are presented in this paper, provide an opportunity for qualitative and quantitative characterization, even at physiologically relevant conditions. Therefore, this work establishes and illustrates, in principle and potential, a simple and novel approach for the development of a voltammetric sensor which is based on the GCE and ITO electrodes.

References

1. N. Yoshioka, K. Ichihashi, *Talanta* 74 (2008) 1408.
2. P.C. Zhang, R.J. Scrudato, J.J. Pagano, R.N. Roberts, *Chemosphere* 26 (1993) 1213.
3. J. Chiarenzelli, R. Scrudato, M. Wunderlich, D. Raerty, K. Jensen, G. Oenga, R. Roberts, J. Pagano, *Chemosphere* 31 (1995) 3259.
4. I.W. Huang, C.S. Hong, B. Bush, *Chemosphere* 32 (1996) 1869.
5. S. Wen, J. Zhao, G. Sheng, J. Fu, P. Peng, *Chemosphere* 50 (2003) 111.
6. P. Huo, Y. Yan, S. Li, H. Li, W. Huang, S. Chen, X. Zhang, *Desalination* 263 (2010) 258.
7. A.Mills, P. Grosshans, E. Snadden, *Sen. Actuators B* 136 (2009) 458.
8. G. McDonnell, A.D. Russell, *Clin. Microbiol. Rev.* 12 (1999) 147.
9. R.C. Peña, J.C. M. Gamboa, M. Bertotti, T.R.L.C. Paixão, *Int. J. Electrochem. Sci.* 6 (2011) 394 – 403.
10. K.C. Lin, T.H. Tsai, S.M. Chen, *Biosens. Bioelectron* 26 (2010) 608-614.
11. Y.C. Wu, R. Thangamuthu, S.M. Chen, *Electroanalysis* 21 (2009) 210.
12. A. Balamurugan, S.M. Chen, *Electroanalysis* 21(2009) 1419 – 1423.

13. A.P. Periasamy, S.W.Ting, S.M. Chen, *Int. J. Electrochem. Sci.* 6 (2011) 2688 – 2709.
14. S. Thiagarajan, T. H. Tsai, S.M.Chen, *Int. J. Electrochem. Sci.* 6 (2011) 2235 – 2245.
15. F.B. Luo, J. Yin, F. Gao, *Microchim. Acta* 165 (2009) 23.
16. A.Tahirovic, A. Copra, E.O. Miklicanin, K. Kalcher, *Talanta* 72 (2007) 1378.
17. B. Tang, Y. Wang, Y. Sun, H.X. Shen, *Spectrochim. Acta A* 58 (2002) 141.
18. P.A. Tanner, A.Y.S. Wong, H. Yuan, R.X. Cai, Z.T. Pan, *Anal. Lett.* 36 (2003) 277.
19. J. Zoua, J. Gao, *J. Hazard. Mater.* 185 (2011) 710.
20. U. Yogeswaran, S. M. Chen, *J. Electrochem. Soc.* 154 (2007) E178.
21. U. Yogeswaran, S. M. Chen, *Sen. Actuators B* 130 (2008) 739.
22. C. Tang, U. Yogeswaran, S. M. Chen, *Anal. Chim. Acta* 636 (2009) 19.
23. K. Jiang, L. S. Schadler,R. W. Siegel, X. Zhang, H. Zhangc and M. Terronesd, *J. Mater. Chem.*14 (2004) 37.
24. K. C. Lin, T. H. Tsai, S. M. Chen, *Biosens. Bioelectron.* 26 (2010) 608.
25. J. Wang, J. Dai, T. Yarlagadda, *Langmuir* 21(2005) 9.
26. M. Tahhan, V. T. Truong, G.M. Spinks, G. G. Wallace, *Smart Mater. Struct.* 12 (2003) 626.
27. T. Komura, G.Y. Niu, T. Yamaguchi, M. Asano, A. Matsuda, *Electroanalysis* 16 (2004) 1791.
28. U. Yogeswaran, S. Thiagarajan, S. M. Chen, *Carbon* 45 (2007) 2783.
29. C. Barbero, M.C. Miras, R. Kotz, O. Hass, *J. Electroanal. Chem.* 437 (1997) 191.
30. E.P. Kovalchuk, S. Whittingham, O.M. Skolozdra, P.Y. Zavalij, I.Y. Zavaliy, O.V. Reshetnyak, M. Seledets, *Mater. Chem. Phys.* 69 (2001) 154.
31. M. Lapkowski, E. M. Genies, *J. Electroanal. Chem.* 279 (1990)157.
32. S. Kaplan, M. Conwell, A. F. Richter, A. G. MacDiarmid, *Macromolecules* 22 (1989) 1669.
33. J. G. Masters, Y. Sun, A. G. MacDiarmid, A. J. Epstein, *Synth. Metals.* 41 (1991) 715.
34. Y. Sun, A. G. MacDiarmid, A. J. Epstein, *J. Chem. Soc. Chem.Commun.* (1990) 529.
35. C. P. Andrieux, O. Haas, J. M. SavGant, *J. Am. Chem. Soc.* 108 (1986) 8175.